CONTROL OF LASER RADIATION PARAMETERS. ACTIVE MEDIA

Control over pulsed operation modes of an erbium-doped fibre laser passively mode-locked via nonlinear polarisation rotation

CONTROL OF LASER RADIATION PARAMETERS. ACTIVE MEDIA https://doi.org/10.1070/QEL17174

Control over pulsed operation modes of an erbium-doped fibre laser passively mode-locked via nonlinear polarisation rotation

I.A. Volkov, V.A. Kamynin, P.A. Itrin, S.N. Ushakov,
K.N. Nishchev, V.B. Tsvetkov

Abstract. **We have experimentally demonstrated the possibility of controlling pulse generation modes of an erbium-doped fibre ring laser operating in the anomalous dispersion regime and passively mode-locked via nonlinear polarisation rotation. It has been shown that individual adjustment of the pump power and intracavity polarisation controllers leads to changes in pulse generation mode, without changing the cavity. We have evaluated the key spectral, temporal and energetic characteristics of the observed pulse generation modes.**

Keywords: *erbium-doped fibre laser, conservative soliton, noise-like pulses, dual-wavelength pulses.*

1. Introduction

Pulsed fibre lasers are widely used in spectroscopy [1, 2], medicine [3, 4], materials processing [5, 6], nonlinear optics [7, 8] and other areas. Currently, the most widespread gain media for fibre lasers are Er^{3+}- and Yb^{3+}-doped fibres [9–14]. There is particular interest in sources of ultrashort pulses, whose generation in fibre lasers is typically due to passive mode-locking. To ensure this regime, use is made of various saturable absorbers, such as graphene [15–17], single-walled carbon nanotubes [18–20], topological insulators [21–24], semiconductor saturable absorber mirrors [25–27] and 'artificial' saturable absorbers that employ nonlinear polarisation rotation (NPR) and nonlinear optical mirrors [28–30].

The physics of mode-locked fibre lasers is determined by a complex interplay between amplification, dispersion and nonlinearity, which leads to a variety of laser operation modes. Experimentally demonstrated phenomena include passive fundamental mode-locking (PFML), pulse splitting, passive harmonic mode-locking and *Q*-switching. Only one pulse circulates in the cavity of a PFML laser. At cavity lengths from a few to tens of metres, the output pulse duration of an erbium fibre laser is typically from tens of femtoseconds to several picoseconds [31, 32]. To obtain nanosecond pulses, the cavity length should be increased to hundreds of metres or even more. Xu et al. [33] demonstrated nanosecond erbium fibre laser operation with the pulse duration varied from 3 to 20 ns at a repetition rate from 1.54 MHz to 200 kHz, respectively, by varying the cavity length. There is evidence that, in addition to usual passive mode-locking states, fibre lasers can generate noise-like pulses, consisting of quasi-stable picosecond wave packets with randomly distributed femtosecond pulses inside [34]. Moreover, recent work has demonstrated a regime in which a new class of pulses are formed – similaritons – which have a parabolic temporal profile with linear frequency modulation [35–37].

In this paper, we examine the feasibility of controlling pulsed operation modes of an erbium-doped all-fibre ring laser by varying the pump power and polarisation controllers, without changing the cavity. We demonstrate spectral, temporal and energetic characteristics of the regimes obtained.

2. Experimental setup

Figure 1 shows a schematic of a fibre ring laser with a cavity length $L \sim 190$ m. The cavity includes a 3-m length of SM-EYDF-6/125-HE Nufern active fibre and a 180-m length of E3 standard single-mode fibre (Optic Fiber Systems JSC, Saransk). The fibre ring laser is pumped by a laser diode (BWT K976F06FA) operating at a wavelength of 976 nm and

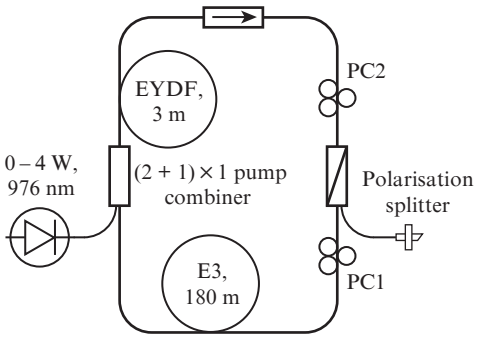

Figure 1. Schematic of the experimental setup:
EYDF, fibre codoped with Er^{3+}/Yb^{3+} ions; E3, standard single-mode fibre; PC1 and PC2, polarisation controllers.

I.A. Volkov, K.N. Nishchev Ogarev Mordovia State University, Bol'shevistskaya ul. 68, 430005 Saransk, Mordovian Republic, Russia; e-mail: emofan_80@mail.ru;
V.A. Kamynin Prokhorov General Physics Institute, Russian Academy of Sciences, ul. Vavilova 38, 119991 Moscow, Russia; e-mail: kamyninva@gmail.com;
P.A. Itrin Ulyanovsk State University, ul. L. Tolstogo 42, 432970 Ulyanovsk, Russia; e-mail: itrin@mail.ru;
S.N. Ushakov Ogarev Mordovia State University, Bol'shevistskaya ul. 68, 430005 Saransk, Mordovian Republic, Russia; Prokhorov General Physics Institute, Russian Academy of Sciences, ul. Vavilova 38, 119991 Moscow, Russia; e-mail: ushserg63@mail.ru;
V.B. Tsvetkov Prokhorov General Physics Institute, Russian Academy of Sciences, ul. Vavilova 38, 119991 Moscow, Russia; National Nuclear Research University MEPhI, Kashirskoe shosse 31, 115409 Moscow, Russia; e-mail: tsvetkov@lsk.gpi.ru

Received 29 October 2019
Kvantovaya Elektronika **50** (2) 153–156 (2020)
Translated by O.M. Tsarev

having an output power of up to 4 W. The pump light is launched into the cavity using a pump combiner with a (2 + 1) × 1 signal fibre. An isolator is used to ensure unidirectional light propagation. A polarisation splitter and two polarisation controllers allow NPR mode-locking to be achieved. Different laser operation modes were ensured by thoroughly adjusting the polarisation controllers. The laser output was connected to a 1 × 3 coupler using an optical plug, which allowed us to simultaneously monitor the spectral and temporal characteristics of the laser.

Optical spectra of output pulses of the fibre ring laser were recorded by an optical spectrum analyser (Yokogawa AQ6370C) in the spectral range 600–1700 nm with a resolution of 0.2 nm. A pulse train was recorded using a high-speed InGaAs PIN photodiode detector (5 GHz) and GWIN-STEK GDS-3000 (500 MHz) and Tektronix MSO 5204 (2 GHz) oscilloscopes. Temporal characteristics of optical pulses were studied using a Femtochrome FR-103WS autocorrelator.

3. Experimental results

At a pump power of 880 mW, after thoroughly adjusting the polarisation controllers we observed the generation of a conservative soliton with spectral sidebands. Figure 2 shows spectral and temporal characteristics of the soliton regime of the fibre laser. Figure 2a presents an optical spectrum of this regime. The centre wavelength in the soliton regime, λ_c, was 1566 nm and the 3-dB bandwidth was 3.6 nm. The pulse repetition rate was 1.1 MHz, which corresponded to the cavity length (Fig. 2a, inset).

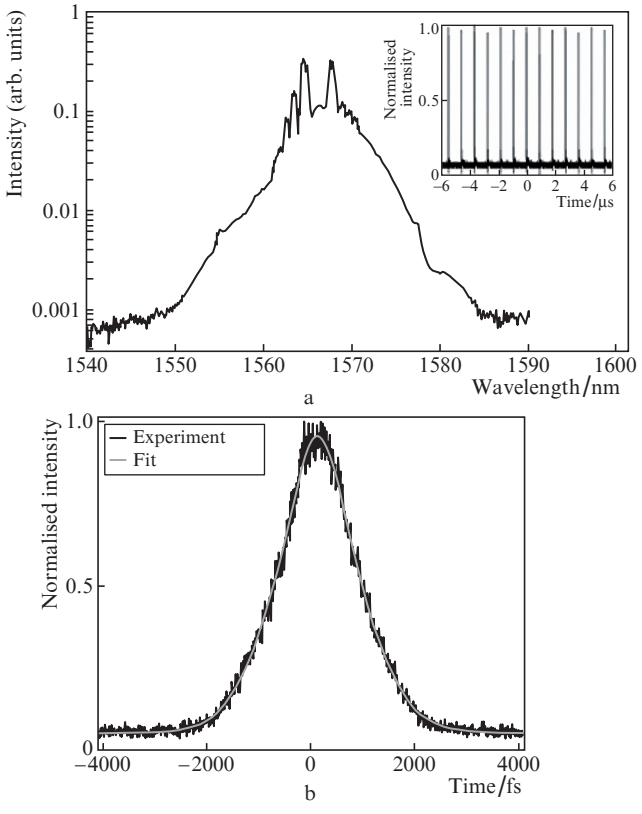

Figure 2. Soliton regime of the laser: (a) optical spectrum and (b) ACT (here and in Figs 3 and 5, the grey solid line represents a sech^2 fit to the pulse profile).

The average output power under such conditions was 14 mW. Figure 2b shows the autocorrelation trace (ATC) of a pulse. Under the assumption that the pulse had a sech^2 profile, its duration was estimated at 1.1 ps. Taking into account Kadel's formula [38] and first-order Kelly peaks, we estimated the intracavity group velocity dispersion: $\beta_2 L = -3.04$ ps^2.

Further raising the pump power to 960 mW and varying the settings of the polarisation controllers, we obtained a broad and smooth laser output spectrum. Figure 3 presents spectral and temporal characteristics of this regime. Figure 3a shows an optical spectrum with a centre wavelength of 1568 nm and 3-dB bandwidth of 15 nm. The inset in Fig. 3a shows a periodic pulse train with a repetition rate of 1.1 MHz.

The ACT in Fig. 3b has the form of a narrow pulse on a broad pedestal. This suggests that the actual mode-locked pulse consists of a train of coherent random narrow peaks. The pulse duration τ is estimated at ~300 fs (with allowance for the sech^2 pulse profile). Such features of the spectrum and ACT are the signature of noise-like pulses. The generation of such pulses is associated with a pulse collapse effect and positive feedback and is a common feature of passively mode-locked soliton fibre lasers [39]. The average power was 21 mW, and the pulse energy was 19 nJ.

Raising the pump power to 1.12 W and adjusting the polarisation controllers, we obtained rectangular nanosecond pulses. The optical spectrum presented in Fig. 4a has the form of a smooth, sharp peak, without spectral sidebands. In this laser operation mode, the centre wavelength was 1567 nm and the 3-dB bandwidth was ~5.7 nm. The corresponding temporal pulse profile is displayed in Fig. 4b.

A rectangular pulse shape was observed in previous studies [40, 41]. Wang et al. [42] accounted for this laser operation mode in terms of a dissipative soliton resonance.

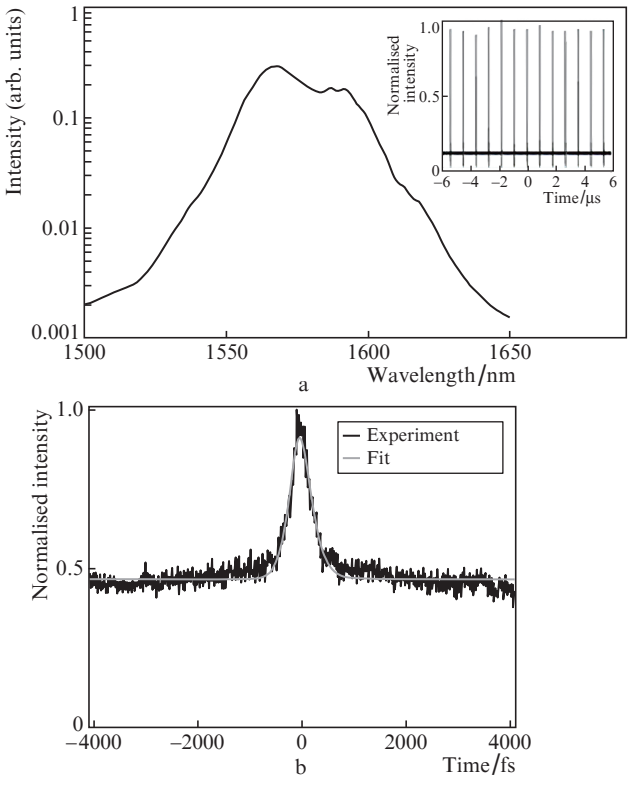

Figure 3. Gaussian noiselike pulse: (a) optical spectrum and (b) ACT.

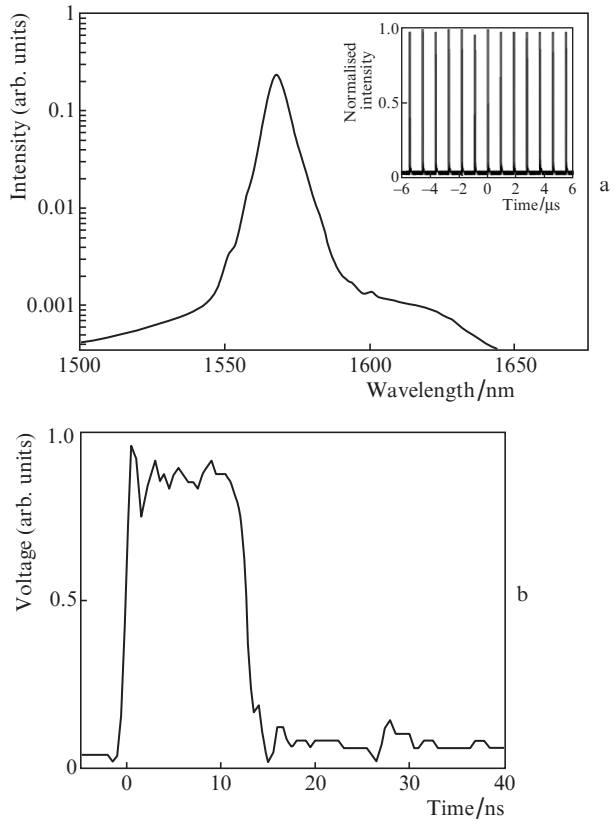

Figure 4. Rectangular noiselike pulse: (a) optical spectrum and (b) temporal profile.

Figure 5 shows an ACT in the form of a sharp peak on a broad pedestal. The average pulse duration is $\tau \approx 1.05$ ps (under the assumption that the pulses have a sech^2 profile). It is worth noting that the pedestal level is related to the density of subpulses in the wave packet and the statistical distribution of their intensity [43]. The average power was 20 mW, and the pulse energy can be estimated at 18 nJ.

Such behaviour can be due to changes in lasing regime switching power [44]. Switching power plays an important role in determining spectral and temporal properties of noise-like pulses. At a low switching point, the peak power stabilises and the laser operates in the conservative soliton regime. If the switching point shifts to higher powers, the pulse becomes unstable and evolves into a noise-like pulse. Therefore, control over this parameter is a convenient way to adjust pulse characteristics: at a given accessible energy, a low switching power limits the rise in pulse peak power, favouring the generation of a large number of pulses with a relatively low peak power and, accordingly, long duration (and narrow spectrum). At a high switching power, the soliton peak power can rise to high values, associated with shorter durations, and, as the energy of individual pulses rises, their number decreases and they form a shorter train.

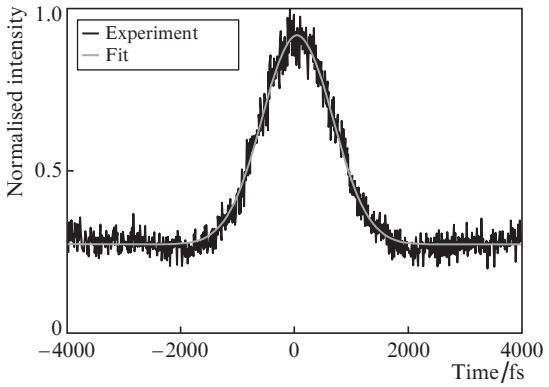

Figure 5. ACT of a rectangular noiselike pulse.

Further raising the pump power to 1.2 W and adjusting the polarisation controllers led to the generation of dual-wavelength pulses. Their optical spectrum is shown in Fig. 6a. The spectral lines peak at 1569 and 1614 nm, with 3-dB linewidths of 6.3 and 5.7 nm, respectively. The temporal pulse profile is displayed in Fig. 6b. The single pulse in the cavity, of 5 ns duration, has a rectangular shape with sharp edges, and its repetition rate is 1.1 MHz. On an oscilloscope with a sampling rate of 2 GHz, no fine pulse structure was detected.

Previously, a spectral doublet was experimentally observed and numerically simulated in a number of studies [45–49]. As shown by Semaan et al. [45], after surpassing the threshold for different laser operation modes with a conservative soliton distribution, one can observe dissipative soliton resonance pulses with a single wavelength and a quasi-Gaussian spectral profile or a spectral doublet of dissipative soliton resonance pulses. In particular, a pump power above 2 W can lead to the generation of a dual-wavelength pulse referred to as a staircase pulse. For example, Zhao et al. [46] described dual-wave-

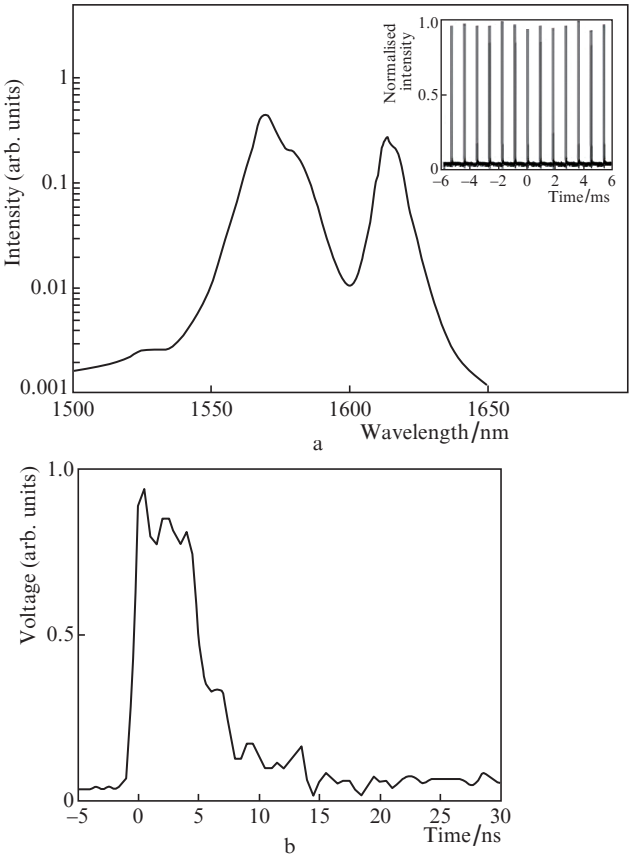

Figure 6. Dual-wavelength pulse generation regime: (a) optical spectrum and (b) temporal pulse profile.

length laser generation of h-shaped and trapezoidal noise-like pulses and investigated their ACFs.

4. Conclusions

We have demonstrated an erbium-doped fibre laser passively mode-locked via NPR, with the possibility of obtaining several laser operation modes by varying the pump power and adjusting intracavity polarisation controllers for each regime. The erbium-doped all-fibre laser has a negative intracavity dispersion and a fundamental pulse repetition rate of 1.1 MHz. The individual adjustment of the pump power and intracavity polarisation controllers has made it possible to achieve pulse generation with various spectral, temporal and energetic characteristics: pulse duration $\tau \approx 1.1$ ps and average power of 14 mW for a conservative soliton with $\lambda_c = 1566$ nm at $\Delta\lambda = 3.6$ nm, pulse duration $\tau \approx 300$ fs and average power of 21 mW for a Gaussian noise-like pulse with $\lambda_c = 1568$ nm at $\Delta\lambda = 15$ nm and pulse duration $\tau \approx 1.05$ ps with an envelope up to 15 ns and average power of 20 mW for a rectangular noise-like pulse with $\lambda_c = 1567$ nm at $\Delta\lambda = 5.7$ nm. We have experimentally demonstrated a transition from the conservative soliton regime to noise-like pulse generation, followed by a transition to dual-wavelength pulses.

Acknowledgements. P.A. Itrin acknowledges the support of the Russian Science Foundation (Grant No. 19-72-100-37).

References

1. Whitenett G., Stewart G., Yu H., Culshaw B. *J. Lightwave Technol.*, **22** (3), 813 (2004).
2. Mehravar S., Norwood R.A., Peyghambarian N., Kieu K. *Appl. Phys. Lett.*, **108**, 231104 (2016).
3. Hoy C. et al. *IEEE J. Sel. Top. Quantum Electron.*, **20** (2), 7100814 (2014).
4. Nagy Z. et al. *J. Cataract Refract. Surg.*, **40**, 20 (2014).
5. Kammel R. et al. *Light Sci. Appl.*, **3**, e169 (2014).
6. Watanabe W., Li Y., Itoh K. *Opt. Laser Technol.*, **78**, 52 (2016).
7. Zheng Z. et al. *Photonics Res.*, **4** (4), 135 (2016).
8. Petersen C. et al. *Nat. Photonics*, **8**, 830 (2014).
9. Okhotnikov O., Grudinin A., Pessa M. *New J. Phys.*, **6**, 177 (2004).
10. Wise F.W., Chong A., Renninger W.H. *Laser Photonics Rev.*, **2**, 58 (2008).
11. Lin K.-H., Kang J.-J., Wu H.-H., Lee C.-K., Lin G.-R. *Opt. Express*, **17**, 4806 (2009).
12. Grelu P., Akhmediev N. *Nat. Photonics*, **6**, 84 (2012).
13. Nishizawa N. *Jpn. J. Appl. Phys.*, **53**, 090101 (2014).
14. Wang J.-Y., Lin K.-H., Chen H.-R. *Opt. Lett.*, **40**, 483 (2015).
15. Sun Z. et al. *ACS Nano*, **4** (2), 803 (2010).
16. Martinez A., Sun Z. *Nat. Photonics*, **7**, 842 (2013).
17. Tarka J. et al. *IEEE J. Sel. Top. Quantum Electron.*, **23** (1), 60 (2017).
18. Wang F. et al. *Nat. Nanotechnol.*, **3**, 738 (2008).
19. Castellani C. et al. *Opt. Lett.*, **36** (20), 3996 (2011).
20. Chernysheva M. et al. *Sci. Rep.*, **7**, 44314 (2017).
21. Zhao C. et al. *Appl. Phys. Lett.*, **101**, 211106 (2012).
22. Liu W. et al. *Sci. Rep.*, **6**, 19997 (2016).
23. Lee J., Koo J., Lee J. *Opt. Eng.*, **55** (8), 081309 (2016).
24. Yan P. et al. *Sci. Rep.*, **5**, 8690 (2015).
25. Wang Q., Geng J., Jiang Z., Luo T., Jiang S. *IEEE Photonics Technol. Lett.*, **23** (11), 682 (2011).
26. Liu S. et al. *IEEE Photonics Technol. Lett.*, **29** (6), 551 (2017).
27. Gomes L., Orsila L., Jouhti T., Okhotnikov O. *IEEE J. Sel. Top. Quantum Electron.*, **10** (1), 129 (2004).
28. Smirnov S., Kobtsev S., Kukarin S. *Opt. Express*, **22** (1), 1058 (2014).
29. Lian Y. et al. *Laser Phys. Lett.*, **14**, 55101 (2017).
30. Olivier M., Gagnon M., Piché M. *Opt. Express*, **23** (5), 6738 (2015).
31. Kuan W.-H., Kao L.-T., Wang J.-Y., Lin K.-H. *Opt. Lett.*, **43** (2), 341 (2018).
32. Jin X., Hu G., Zhang M., Hu Y., Albrow-Owen T., Howe R.C.T., Wu T.-C., Wu Q., Zheng Z., Hasan T. *Opt. Express*, **26** (10), 12506 (2018).
33. Xu J., Wu S.D., Liu J., Wang Q., Yang Q.-H., Wang P. *Opt. Commun.*, **285**, 4466 (2012).
34. Liu J., Chen Y., Tang P., Xu C., Zhao C., Zhang H., Wen S. *Opt. Express*, **23** (5), 6418 (2015).
35. Oktem B., Ülgüdür C., Ilday F.O. *Nat. Photonics*, **4**, 307 (2010).
36. Chong A., Wright L.G., Wise F.W. *Rep. Prog. Phys.*, **78** (11), 3901 (2015).
37. Zolotovsky I.O., Yavtushenko M.S., Sementsov D.I., Yavtushenko I.O., Sysoliatin A.A., Okhotnikov O.G. *Proc. SPIE*, **7917**, 79171T (2011).
38. Kadel R., Washburn B.R. *Appl. Opt.*, **51** (27), 6465 (2012).
39. Pottiez O., Grajales-Coutiño R., Ibarra-Escamilla B., Kuzin E.A., Hernández-García J.C. *Appl. Opt.*, **50** (25), E24 (2011).
40. Zhao G.-K., Chen H.-J., Liu H.-Z., Chen W.-C., Luo A.-P., Xing X.-B., Cui H., Luo Z.-H., Xu W.-C. *Opt. Express*, **26** (14), 17804 (2018).
41. Pottiez O., Grajales-Coutiño R., Ibarra-Escamilla B., Kuzin E.A., Hernández-García J.C. *Laser Phys.*, **24** (11), 5103 (2014).
42. Wang S.K., Ning Q.Y., Luo A.P., Lin Z.B., Luo Z.C., Xu W.C. *Opt. Express*, **21** (2), 2402 (2013).
43. Lauterio-Cruz J.P., Pottiez O., Bracamontes-Rodríguez Y.E., Hernández-García J.C., García-Sánchez E., Bello-Jimenez M., Kuzin E.A. *Laser Phys.*, **27** (6), 065107 (2017).
44. Tang D.Y., Zhao L.M., Zhao B. *Opt. Express*, **13**, 2289 (2005).
45. Semaan G., Komarov A., Niang A., Meng Y., Kemel M., Salhi M., Sanchez F. *Phys. Res. A*, **97**, 023812 (2018).
46. Zhao N., Liu M., Liu H., Zheng X., Ning Q., Luo A., Luo Z., Xu W. *Opt. Express*, **22** (9), 10906 (2014).
47. Zhang C., Zhao J.F., Miao C.Y. *Laser Phys.*, **22** (10), 1573 (2012).
48. Kuzmenkov A.I., Lukinykh S.N., Nanii O.E., Odintsov A.I., Smirnov A.P., Fedoseev A.I., Treshchikov V.N. *Quantum Electron.*, **46** (9), 795 (2016) [*Kvantovaya Elektron.*, **46** (9), 795 (2016)].
49. Nanii O.E., Odintsov A.I., Smirnov A.P., Fedoseev A.I. *Moscow Univ. Phys. Bull.*, **71** (4), 389 (2016).